Two Flavoenzymes Catalyze the Post-Translational Generation of 5-Chlorotryptophan and 2-Aminovinyl-Cysteine during NAI-107 Biosynthesis

Manuel A. Ortega,[†] Dillon P. Cogan,[†] Subha Mukherjee,[‡] Neha Garg,[†] Bo Li,[†] Gabrielle N. Thibodeaux,[‡] Sonia I. Maffioli,[§] Stefano Donadio,[§] Margherita Sosio,[§] Jerome Escano,[∥] Leif Smith,[∥] Satish K. Nair,*[,†,⊥] and Wilfred A. van der Donk*[,†,‡,#]

[†]Department of Biochemistry, University of Illinois at Urbana—Champaign, Roger Adams Laboratory, 600 S. Mathews Ave., Urbana, Illinois 61801, United States

[‡]Department of Chemistry, University of Illinois at Urbana—Champaign, Roger Adams Laboratory, 600 S. Mathews Ave., Urbana, Illinois 61801, United States

[§]NAICONS Srl, Viale Ortles 22/4, 20139 Milan, Italy

[∥]Department of Biology, Texas A&M University, Butler Hall 100, 3258 TAMU, College Station, Texas 77843, United States

[⊥]Center for Biophysics and Computational Biology, University of Illinois at Urbana—Champaign, Roger Adams Laboratory, 600 S. Mathews Ave., Urbana, Illinois 61801, United States

[#]Howard Hughes Medical Institute, University of Illinois at Urbana—Champaign, Roger Adams Laboratory, 600 S. Mathews Ave., Urbana, Illinois 61801, United States

S Supporting Information

ABSTRACT: Lantibiotics are ribosomally synthesized and post-translationally modified antimicrobial peptides containing thio-ether rings. In addition to these cross-links, the clinical candidate lantibiotic NAI-107 also possesses a C-terminal S-[(Z)-2-amino-vinyl]-D-cysteine (AviCys) and a unique 5-chloro-L-tryptophan (ClTrp) moiety linked to its potent bioactivity. Bioinformatic and genetic analyses on the NAI-107 biosynthetic gene cluster identified *mibH* and *mibD* as genes encoding flavoenzymes responsible for the formation of ClTrp and AviCys, respectively. The biochemical basis for the installation of these modifications on NAI-107 and the substrate specificity of either enzyme is currently

unknown. Using a combination of mass spectrometry, liquid chromatography, and bioinformatic analyses, we demonstrate that MibD is an FAD-dependent Cys decarboxylase and that MibH is an FADH$_2$-dependent Trp halogenase. Most FADH$_2$-dependent Trp halogenases halogenate free Trp, but MibH was only active when Trp was embedded within its cognate peptide substrate deschloro NAI-107. Structural comparison of the 1.88-Å resolution crystal structure of MibH with other flavin-dependent Trp halogenases revealed that subtle amino acid differences within the MibH substrate binding site generates a solvent exposed crevice presumably involved in determining the substrate specificity of this unusual peptide halogenase.
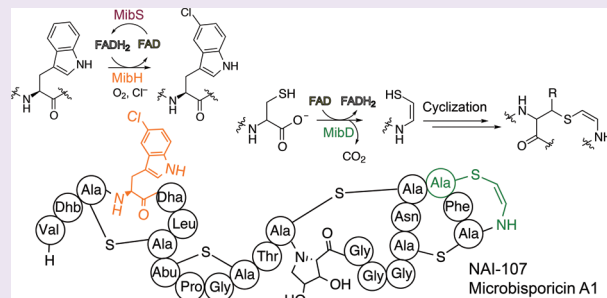
R ibosomally synthesized and post-translationally modified peptides (RiPPs) are a growing class of natural products containing a wide array of unique pharmacophores.[1] These moieties are introduced on a ribosomally synthesized precursor peptide by dedicated biosynthetic enzymes[2] and bestow upon these molecules their biological activities. As such, character-ization of RiPP biosynthetic enzymes provides an avenue to harness the potential of these catalysts as tools for the development of chemoenzymatic methodologies to generate novel therapeutic peptides.

Within RiPPs, lanthipeptides (lanthionine-containing pep-tides) encompass one of the most abundant and well-studied subfamilies to date.[1] The key structural features defining lanthipeptides are thioether rings formed by the bis-amino acids

lanthionine (Lan) and/or methyllanthionine (MeLan; Figure 1a). These cross-links are introduced enzymatically *via* dehydration of select Ser/Thr residues to 2,3-dehydroalanine (Dha) and (Z)-2,3-dehydrobutyrine (Dhb), respectively, within the C-terminal core region of a precursor peptide (LanA), followed by subsequent Michael-type additions of Cys thiols onto the newly generated dehydroamino acids (Figure 1a).[3,4] The enzymes responsible for catalyzing both modifications require an N-terminal leader peptide sequence within the precursor peptide for efficient processing.[5−7] After thioether
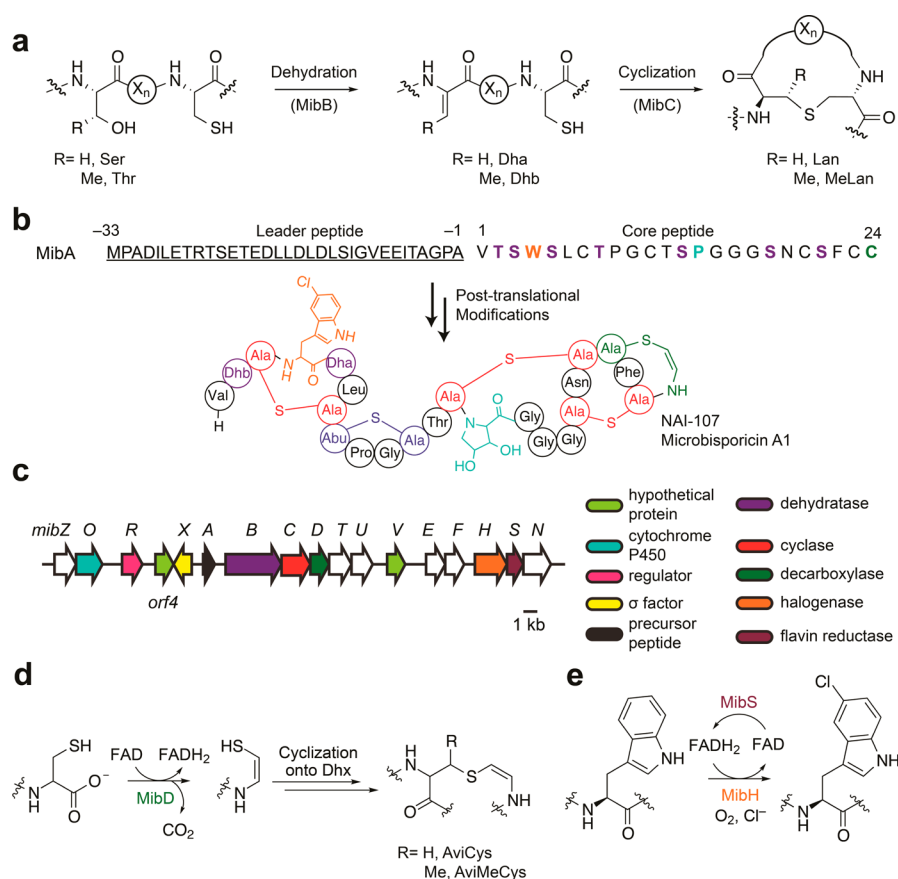
Figure 1. Overview of NAI-107 biosynthesis. (a) Scheme for thioether ring formation during lanthipeptide biosynthesis. The enzymes that catalyze each step during NAI-107 biosynthesis are shown in parentheses. (X$_n$) connecting peptide. (b) Structure of NAI-107. The amino acid sequence of the precursor peptide MibA is shown. Negative numbers represent the position of amino acids within the leader peptide (underlined) with respect to the first amino acid in the core region. Dehydroamino acids, lanthionine, and methyllanthionine are shown in purple, red, and blue, respectively. The aminovinyl cysteine and 5-chlorotryptophan are colored green and orange. NAI-107 also contains a 3,4-dihydroxyproline moiety shown in cyan. (c) NAI-107 biosynthetic gene cluster. (d,e) Proposed reactions catalyzed by the enzymes (d) MibD and (e) MibH/MibS. Dhx, dehydroalanine or dehydrobutyrine; AviMeCys, S-[(Z)-2-aminovinyl]-(3S)-3-methyl-D-cysteine.

ring formation, one or more proteases remove the N-terminal leader sequence from the precursor peptide releasing the mature natural product. Lanthipeptides exhibiting antimicrobial activity are known as lantibiotics (lanthionine-containing antibiotics).

In addition to these common post-translational modifications, some lanthipeptides contain additional modified residues installed by tailoring enzymes. These modifications in many cases increase the stability and biological activity of the peptides. For instance, epilancin 15X contains an N-terminal lactate that serves to protect it against the action of aminopeptidases.[8] Similarly, the lantibiotic NAI-107 (also known as microbisporicin) contains a C-terminal AviCys predicted to arise from the oxidative decarboxylation of a Cys residue within the NAI-107 precursor peptide (Figure 1b).[9] Presumably, this modification protects the peptide from carboxypeptidases and removes a negative charge, which has proven beneficial for bioactivity in semisynthetic lanthipeptide analogs.[10] In addition, NAI-107 contains a 3,4-dihydroxyproline (diHPro) and a unique ClTrp responsible for increasing its bioactivity 2-fold compared to its deschloro counterpart (Figure 1b).[9,11] The benefits these additional modifications confer to the stability and bioactivity of lantibiotics prompted biochemical characterization of the tailoring enzymes responsible for installing AviCys and ClTrp during NAI-107 biosynthesis.

NAI-107 is a produced by the actinomycete *Microbispora* sp. 107891.[9,12] NAI-107 acts as a peptidoglycan biosynthesis inhibitor by sequestering the cell wall precursor lipid II and is currently in preclinical trials for the treatment of multidrug resistant Gram-positive bacterial infections.[13−15] NAI-107 biosynthesis commences with the translation of the precursor peptide MibA (Figure 1b).[12,16] Then, MibB dehydrates seven Ser/Thr residues within the core region of MibA in a glutamyl-tRNA^{Glu}-dependent manner, and the lanthipeptide cyclase MibC catalyzes the nucleophilic addition of Cys residues onto five dehydroamino acids.[17] The biosynthetic details regarding AviCys, ClTrp, and diHPro installation during NAI-107 biosynthesis are not known.

Previous bioinformatic and genetic analyses of the NAI-107 biosynthetic gene cluster identified two genes coding for enzymes predicted to be responsible for the decarboxylation and halogenation (Figure 1c).[12] One of the open reading frames (ORFs), *mibD*, encodes an enzyme that has sequence similarity to lanthipeptide decarboxylases (LanD).[18,19] These enzymes together with (R)-4′-phospho-N-pantothenoylcysteine (PPC) decarboxylases belong to the homo-oligomeric flavin-containing Cys decarboxylase (HFCD) superfamily that employs a flavin cofactor to catalyze the oxidative decarboxylation of C-terminal Cys-containing peptides (Figure 1d).[18−20] Decarboxylation proceeds via oxidation of a Cys thiol to a

thioaldehyde that subsequently serves to delocalize the negative charge developed at the former Cα upon decarboxylation.[21−25] Nucleophilic addition of the C-terminal aminoenethiolate to a nearby dehydroamino acid within the core peptide yields the AviCys moiety (Figure 1d).[25] At present, it is unclear whether this latter reaction is catalyzed by lanthipeptide decarboxylases or lanthipeptide cyclases or if it proceeds nonenzymatically.

A second ORF, *mibh*, shows homology to flavin-dependent Trp halogenases.[12] Members of this enzyme class (Figure 1e) use reduced flavin to activate molecular oxygen.[26] A halide ion is believed to perform a nucleophilic attack onto the distal oxygen atom of a 4a-flavin hydroperoxide forming a hypohalite that subsequently transfers the halogen to a nearby conserved Lys residue (Lys102 in MibH). This chloramine intermediate is then believed to halogenate Trp.[27−29] Within the NAI-107 biosynthetic gene cluster, *mibS* encodes a protein that shows sequence similarity to flavin reductases and is presumably responsible for providing reduced flavin to MibH (Figure 1e).[12]

In this study, we reconstituted the activity of MibD, MibS, and MibH *in vitro*. Decarboxylation assays revealed MibD to be specific for the C-terminal sequence in the precursor peptide MibA and to not require the N-terminal leader peptide for activity. MibH and MibS form an FAD-dependent halogenase system. Interestingly, halogenation assays with a panel of different substrate analogs revealed MibH to be highly specific for the modified MibA core peptide carrying thioether rings suggesting halogenation to occur in one of the last steps of NAI-107 biosynthesis. Last, the 1.88-Å-resolution crystal structure of holo MibH provides a structural basis for its unusual substrate specificity.

■ RESULTS AND DISCUSSION

***In Vitro* Reconstitution of MibD As a Lanthipeptide Cys Decarboxylase.** The gene encoding MibD was heterologously expressed in *Escherichia coli* as a hexahistidine (His$_6$) tagged protein and purified *via* immobilized metal affinity chromatography. To identify the type of flavin, the purified protein was heat-denatured, the flavin was isolated *via* reversed phase solid phase extraction and analyzed using matrix-assisted laser desorption/ionization time-of-flight mass spectrometry (MALDI-TOF MS), revealing a mass of 782.81 Da, consistent with FAD (Supporting Information Figure S1). The isolation of FAD from His$_6$-MibD suggests the cofactor is not covalently linked.

To reconstitute MibD activity *in vitro*, enzyme assays were performed with the linear precursor peptide His$_6$-MibA as a substrate, resulting in the appearance of a lower molecular weight product as observed by MALDI-TOF MS (Figure 2a). To determine if the MibA leader peptide was required for MibD activity, enzyme assays were performed using the MibA core peptide as substrate resulting again in the formation of a new product displaying a mass loss consistent with an oxidative decarboxylation event (Figure 2b). Tandem MS/MS analysis of the product localized the modification to the C-terminus of the core peptide (Figure 2c) in agreement with the formation of an aminoenethiolate moiety from a C-terminal Cys residue.[18,19,25,30] Thus, in contrast to lanthipeptide dehydratases and cyclases, MibD activity is not dependent on a leader peptide. The absence of starting material following the activity assays (Figure 2a,b) suggests that MibD activity is not coupled to an oxidoreductase responsible for oxidizing FADH$_2$. Instead, the results imply that the reduced flavin generated upon oxidative decarboxylation must have been reoxidized by O$_2$.
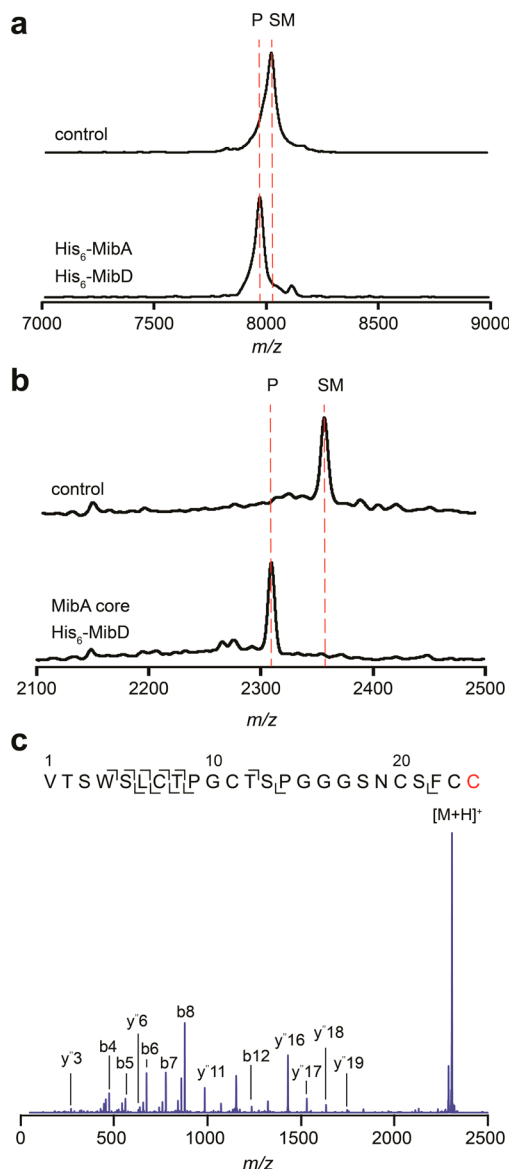

Figure 2. *In vitro* reconstitution of His$_6$-MibD activity. (a,b) MALDI-TOF MS analysis of oxidative decarboxylation reactions after incubation with His$_6$-MibD and (a) His$_6$-MibA or (b) MibA core peptide. Top mass spectra represent a control reaction performed in the absence of His$_6$-MibD. Bottom mass spectra represent a reaction containing His$_6$-MibD. SM, starting material; P, product. (c) ESI-Q/TOF tandem MS fragmentation analysis of MibA core peptide after modification by His$_6$-MibD. Cys modified by MibD is shown in red. The y ions carrying a difference of 46 Da suggests modification occurs at the C-terminus. For (a) SM, average mass calcd. [M + H]$^+$, 8013; obsd., 8022. P, average mass calcd. [M + H]$^+$, 7967; obsd., 7971. For (b) SM, average mass calcd. [M + H]$^+$ 2355, obsd. 2356; P, average mass calcd. [M + H]$^+$ 2309, obsd. 2309. For (c) precursor parent ion, monoisotopic mass calcd. [M + H]$^+$, 2307.90; obsd., 2307.93.

Finally, the observation that MibD is capable of utilizing the precursor peptide MibA lacking dehydrations and thioether rings as substrate suggests that these post-translational modifications are not important for mediating substrate recognition by MibD and that, *in vivo*, MibD may act first. The observation that MibD efficiently decarboxylates linear MibA is similar to reports on EpiD and MrsD involved in oxidative decarboxylation during the biosynthesis of epidermin and mersacidin, respectively.[19,31,32] To unambiguously test
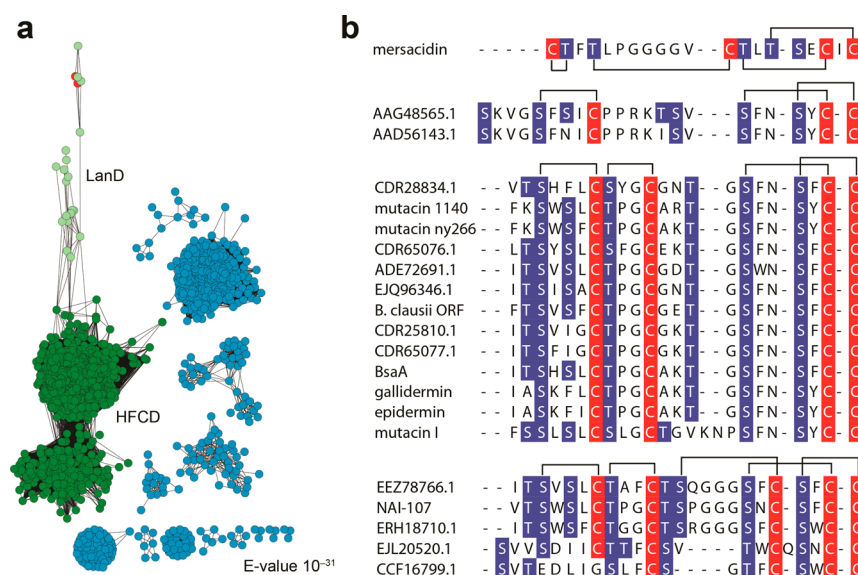
Figure 3. Substrate sequences of lanthipeptide decarboxylases. (a) Sequence similarity network of PFAM 02441 at a 60% sequence identity for each node. The HFCD superfamily cluster is shown in green. The LanD subcluster is colored light green. HFCD enzymes involved in the biosynthesis of holomycin and tropodithietic acid are shown in red. Other subfamilies are colored light blue. (b) Sequence alignment of select lanthipeptide precursor peptides from gene clusters containing lanthipeptide decarboxylases. Dehydratable residues are shown in blue, and Cys residues are shown in red. Putative ring topologies are drawn on top of each group based on the topology of characterized lanthipeptides.

whether the LanD proteins act first, kinetic comparisons would be needed between linear peptide and intermediates with various post-translational modifications installed, which are currently inaccessible. Some indication that LanD proteins may act on partially modified peptides *in vivo* comes from a study on MutD, the LanD enzyme involved in mutacin 1140 biosynthesis. MutD was reported to be less efficient *in vivo* when the B-ring was disrupted.[33]

Insights into the Substrate Specificity of Lanthipeptide Decarboxylases. The successful *in vitro* reconstitution of MibD activity prompted us to investigate its potential utility for decarboxylation of noncognate lanthipeptide precursor peptides containing C-terminal Cys residues (Supporting Information Table S1).[34] Under a range of experimental conditions, His$_6$-MibD was only active on its cognate substrate His$_6$-MibA and did not act on other lanthipeptide precursor peptides ending in FTINVC (ProcA1.1), LVGKMC (ProcA1.7), and YWEGEC (ProcA2.8; Supporting Information Table S1).

To obtain further insights into the substrate specificity, a sequence similarity network of the entire flavoprotein superfamily to which MibD belongs (PFAM02441) was built at an expected (E)-value cutoff of 10^{-31}.[35] Within the HFCD superfamily cluster (Figure 3a, green), lanthipeptide decarboxylases formed a separate subgroup (Figure 3a, light green) from PPC-decarboxylases, which are involved in the decarboxylation of PPC during coenzyme A biosynthesis.[20] Interestingly, in addition to lanthipeptide decarboxylases, this subcluster also contained enzymes involved in the biosynthesis of the cysteine-derived sulfur-containing antibiotics holomycin and tropodithietic acid (Figure 3a, red). For both cases, these HFCD enzymes are predicted to catalyze key oxidative sulfur transformations.[36,37]

Close inspection of the precursor peptides associated with each lanthipeptide decarboxylase revealed that these LanA's can be classified into three different groups based on their putative ring topologies (Figure 3b). Irrespective of the group, with the exception of mersacidin, each substrate peptide has a similar C-terminal ring topology with the consensus sequence S-(F/W/N)-(N/C)-S-(F/Y/W/N)-C-C (Figure 3b). The conservation within this sequence suggests that lanthipeptide decarboxylases have evolved to recognize this motif and not only the C-terminal Cys. The noncognate substrates investigated in this study that failed to be decarboxylated do not contain this motif (Supporting Information Table S1), and the observed lack of activity with MibD supports its importance. Two additional lanthipeptide decarboxylases have been structurally and biochemically characterized *in vitro*, EpiD and MrsD.[18,19,23,24,30,38] Similar to MibD, MrsD did not demonstrate appreciable substrate tolerance.[19] In contrast, EpiD was capable of decarboxylating a variety of substrates containing the C-terminal sequence (V/I/L/M/F/Y/W)-(A/S/V/T/C/I/L)-C.[32] Hence, EpiD (or its homologue GdmD)[39] appears to be a better prospect for synthetic biology applications.

MibS Is an NADH-Dependent Flavin Reductase. To probe whether MibS is responsible for supplying the electrons required for NAI-107 halogenation, *mibS* was heterologously expressed as a His$_6$-tagged construct in *E. coli* and reconstituted *in vitro*. Initial expression attempts of the 20.9 kDa reductase resulted in insoluble protein. Coexpression of *mibS* together with the *E. coli* chaperones *groES/EL* afforded soluble protein.[40] Upon purification, the His$_6$-MibS UV/vis absorption spectrum revealed two absorption maxima at 380 and 452 nm, characteristic of oxidized flavoproteins (Supporting Information Figure S2). The bound flavin cofactor was isolated and identified as FAD *via* liquid chromatography electrospray ionization quadrupole time-of-flight mass spectrometry (LC/ESI-Q/TOF MS; Figure S2). NAD(P)H oxidation assays showed His$_6$-MibS to be highly specific for NADH as the electron donor with an apparent K_M of 80 μM and apparent k_{cat} of 198 min^{-1} (Figure S2). The successful reconstitution of MibS as an NADH-dependent FAD reductase allowed the development of enzyme assays to probe the chlorination reaction presumably catalyzed by MibH.
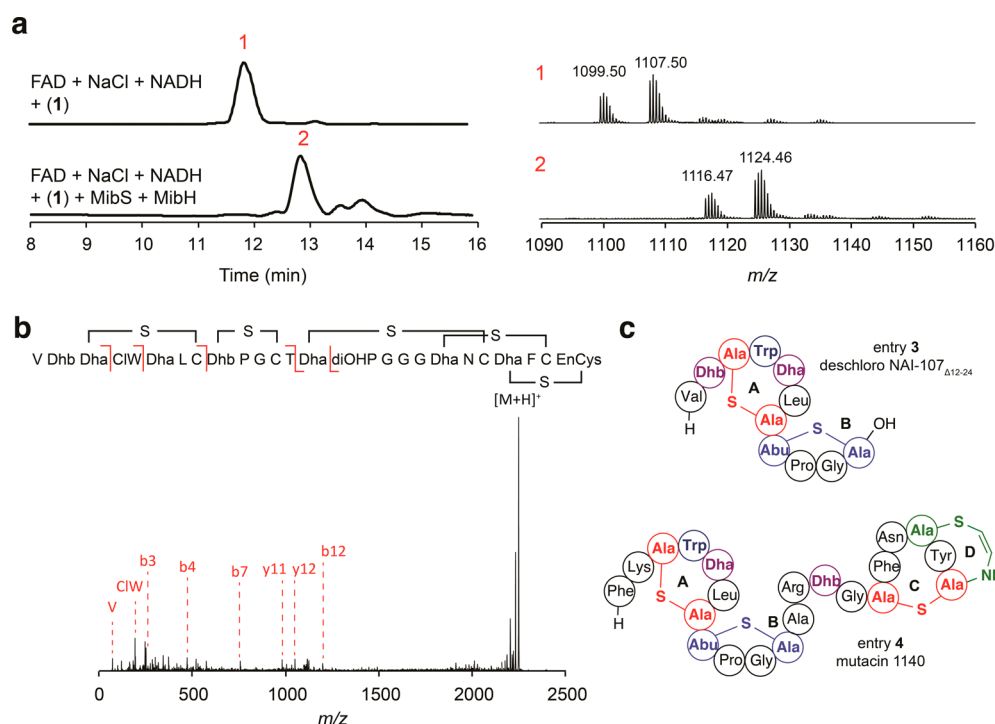
Figure 4. *In vitro* reconstitution of His₆-MibH activity. (a) LC/ESI-Q/TOF MS analysis of halogenation reactions catalyzed by MibH. (Left) Total ion chromatogram (TIC) of halogenation reactions performed in the presence (bottom) or absence (top) of His₆-MibH. The red number on top of each peak serves as an identifier. Starting material (peak 1). Expected chlorinated product (peak 2). Starting material was provided as a mixture of hydroxylated deschloro NAI-107 congeners.[11] (Right) ESI-Q/TOF MS analysis corresponding to each peak identified on the TIC. Black numbers on top of each family of peaks represent the $[M+2H]^{2+}$ monoisotopic m/z values. Monohydroxylated, deschloro NAI-107 monoisotopic mass calcd. $[M+2H]^{2+}$, 1099.41; bishydroxylated deschloro NAI-107 monoisotopic mass calcd. $[M+2H]^{2+}$, 1107.41; monohydroxylated NAI-107, monoisotopic mass calcd. $[M+2H]^{2+}$, 1116.39; bishydroxylated NAI-107, monoisotopic mass calcd. $[M+2H]^{2+}$, 1124.39. (b) ESI-Q/TOF tandem MS/MS fragmentation analysis of deschloro NAI-107 after modification by His₆-MibH. NAI-107 monoisotopic mass calcd. $[M + H]^+$, 2247.77; obsd., 2248.78. Fragmentation inside the N-terminal ring has also been observed for the lantibiotic nisin, and the planosporicin-like family of lantibiotics.[10] ClW, chlorotryptophan; diOHP, dihydroxyproline; EnCys, aminovinylcysteine. (c) Structural representation of substrates **3** and **4**. Color scheme is the same as in Figure 1. Thioether rings are labeled with alphabet letters.

MibH Is an FADH₂-Dependent Halogenase Responsible for ClTrp Formation. Similar to His₆-MibS, soluble protein was only obtained after coexpression of *mibH* with the chaperones *groES/EL*. Flavin was not present following downstream purification, suggesting the enzyme has a weak binding affinity toward its cofactor. Similar results have been observed for other FADH₂-dependent Trp halogenases.[26,27]
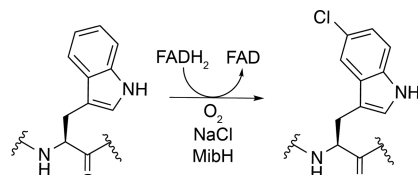
Previous transcriptomic analysis of the NAI-107 native producer *Microbispora corallina* NRRL 30420 indicated that NAI-107 biosynthesis commences with the production of deschloro-deshydroxyl NAI-107.[16] Deschloro-deshydroxyl NAI-107 activates a dedicated sigma factor needed for the transcription of additional NAI-107 biosynthetic genes including *mibH*.[16] Thus, MibH presumably acts at a later stage of NAI-107 biosynthesis, chlorinating the cyclized MibA core. Initial MibH activity assays were therefore carried out using deschloro NAI-107 (**1**) as a substrate. LC/ESI-Q/TOF MS analysis of halogenation assays performed with MibH, MibS, FAD, NADH, NaCl, and **1** revealed the formation of a product peak containing the characteristic mass and isotopic distribution of chlorine-containing compounds (Figure 4a and Figure S3). No chlorinated product was observed when either MibS or MibH was omitted from the reaction assay (e.g., Figure 4a). Furthermore, tandem MS characterization of the chlorinated product revealed chlorination occurred at Trp4 (Figure 4b). Together, our results suggest MibH to be an unusual FADH₂-dependent Trp halogenase capable of chlorinating Trp within peptides.

Characterization of the Substrate Specificity of MibH. All flavin-dependent halogenases characterized to date halogenate free Trp, Trp analogs, or substrates bound to coenzyme A or peptidyl carrier proteins (PCP).[41−44] To determine the substrate specificity of MibH, halogenation assays were performed using free Trp. Regardless of the conditions tested, halogenation activity was not detected (Table 1). This result suggests that MibH only recognizes Trp within the context of a peptide backbone, thus making this enzyme, to the best of our knowledge, the first characterized halogenase exhibiting specificity for Trp within a polypeptide.

We next evaluated the potential of using MibH as a general peptide Trp halogenase. Its activity was tested using several NAI-107 analogs containing a varying degree of post-translational modifications, including the unmodified precursor peptide MibA (**2**) and deschloro NAI-107₍Δ12−24₎ (**3**), a synthetic NA1-107 variant composed of only the first two N-terminal rings (Figure 4c and Supporting Information Figure S4). Surprisingly, given the substrate tolerance of other lanthipeptide tailoring enzymes, MibH was not capable of chlorinating either substrate under the conditions tested as observed by MALDI-TOF MS (Table 1). Intrigued by these results, we then investigated the capability of MibH to chlorinate mutacin 1140 (**4**), another antimicrobial lanthipeptide. Mutacin 1140 contains a Trp residue in the A-ring at the same position as

Table 1. Substrates Tested for Halogenation by MibH

entry	substrate	activity[a]
	Trp	−
1	deschloro NAI-107	+
2	linear His$_6$-MibA precursor peptide	−
3	deschloro NAI-107$_{\Delta 12-24}$	−
4	mutacin 1140	−
	mutacin 1140 F1G	−
	mutacin 1140 K2A	−

[a]Active (+), inactive (−).

1 and shares an analogous overall structural topology with identical A and B rings (Figure 4c).[33,45,46] Despite the high structural similarity to **1**, no chlorination activity was detected with **4** (Table 1). MibH also did not act on the mutacin mutants F1G and K2A (Table 1).[46] Collectively, our results indicate that the different post-translational modifications present in **1** as well as the overall structure of the cyclized compound including its C-terminal rings appear to determine the substrate specificity of MibH. The observation that the enzyme does not require the leader peptide on MibA is consistent with a growing number of RiPP tailoring enzymes that specifically recognize the macrocyclic scaffold and act late in a biosynthetic pathway. Chlorination after the rings are already installed is also consistent with the aforementioned observation wherein nonchlorinated NAI-107 produced earlier in the growth phase activates expression of *mibH*.[16] These results also suggest that chlorination takes place after the removal of the leader peptide. This would require leader peptide cleavage in the cytosol since MibH does not contain any export signal. The protease(s) that removes the leader peptide during the biosynthesis of NAI-107 is currently not known.

Structural Characterization of MibH. To determine the structural basis of such unusual peptide specificity, the crystal structure of MibH bound to FAD was determined to 1.85-Å resolution (Figure 5a and Supporting Information Table S2). MibH crystallized with four molecules in the asymmetric unit, and clear density corresponding to FAD and chloride ions was observed (Figure 5b) in two out of four of these molecules, whereas spurious electron density was observed for the other two molecules. The overall structure of the MibH monomer consists of a large single domain consisting of a rectangular arrangement of several α-helices surrounding two β-sheets, with a triangular helical protuberance appended to the base of this rectangle. The FAD cofactor is positioned in a solvent exposed groove, roughly parallel to the main body of each monomer, with the adenosine moiety positioned near one set of β-strands and the isoalloxazine ring situated at the other set of β-strands. MibH contains two signatures motifs that are conserved among other FADH$_2$-dependent halogenases. The WxWxIP (Trp283-Pro288) motif, whose role in halogenation remains elusive,[47] and the GxGxxG (Gly36-Gly41) flavin consensus sequence that is located in the vicinity of the FAD. A Lys/Glu pair that is catalytically relevant in other FADH$_2$-dependent halogenases is
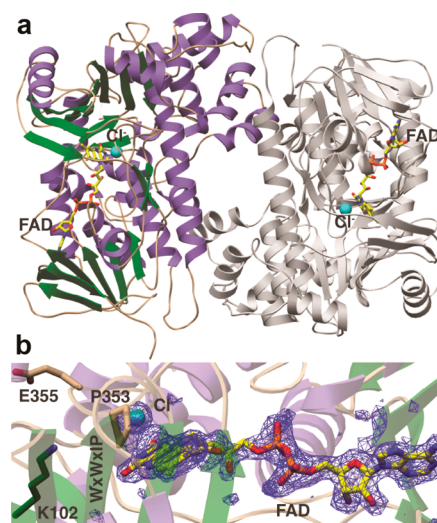

Figure 5. Crystal structure of the lantibiotic halogenase MibH. (a) Overall cartoon representation of MibH. α helices are shown in purple. β sheets are shown in green. Flexible loops are shown in wheat, and the second protomer is shown in gray. FAD and the Cl⁻ ion are shown as sticks and as a cyan sphere, respectively. (b) Simulated annealing omit difference Fourier map ($F_o − F_c$) contoured to 2.5σ of FAD and Cl⁻. The conserved Lys/Glu pair involved in chlorination is shown as sticks. The conserved WXWXIP motif is labeled in one amino acid code.

also present in MibH (Lys102 and Glu355). In orthologous enzymes, the substrate Trp is located more than 10 Å away from the flavin and chlorination of the equivalent Lys facilitates halogenation *via* a covalent Lys chloramine intermediate.[29] The conserved Glu may either facilitate proton abstraction from the Trp substrate following halogenation[26] or enhance the electrophilicity of the chloramine. Electron density corresponding to a chloride ion is located at a pocket at the *Re* face of the isoalloxazine, where it interacts with the backbone amides of Ser357 and Gly358. Pro353 forms the opposing edge of the binding pocket (Figure 5b). As in other FADH$_2$-dependent halogenases, the size of the binding pocket likely precludes the binding of halides such as iodide, but not bromide, consistent with the ability to purify brominated NAI-107 variants when the natural producer is supplemented with bromide sources.[48]

Comparison of MibH with other enzymes in the protein data bank (PDB) *via* the Dali server reveals a conserved global architecture shared among other Trp halogenases. The closest structural relatives to MibH include the 5-Trp halogenase PyrH involved in pyrroindomycin biosynthesis,[49] and the 7-Trp halogenases PrnA and RebH from pyrrolnitrin and rebeccamycin biosynthesis, respectively,[26,27] all of which utilize free Trp as a substrate but exhibit different regioselectivity. Visual inspection of the proposed MibH active site based on conservation of important catalytic residues and the spatial arrangement of FAD and chloride reveals that MibH has a noticeable larger accessible surface area in comparison to free-tryptophan utilizing halogenases, which likely serves to accommodate its larger peptidic substrate (Figure 6a). Interestingly, the similar structural topology of MibH to other FADH$_2$-dependent Trp halogenases suggests this larger crevice did not arise due to structural deletions. Instead, subtle amino acid variations within MibH are responsible for forming the cavity, as revealed by pairwise structural alignments of MibH with different members of this enzyme family.
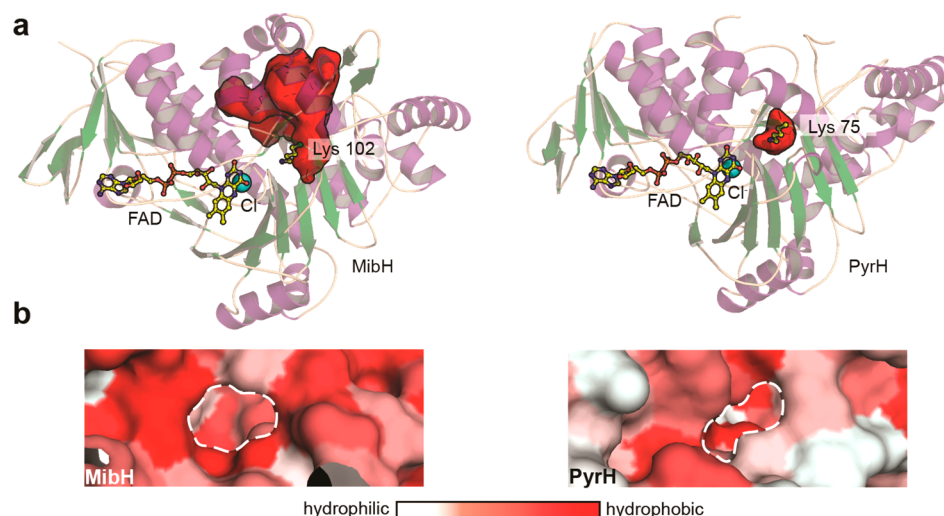
Figure 6. Insights into the substrate specificity of the 5-tryptophan halogenase MibH. (a) Cartoon representation of the overall structure of (left) MibH and (right) PyrH[49] (PDB 2WET) with their respective substrate binding clefts shown as red surfaces. Color scheme is the same as in Figure 5. (b) Surface representation of the proposed Trp binding site (dashed white line) in (left) MibH and (right) PyrH colored by hydrophobicity.

In the absence of a substrate-bound structure, we propose this region to serve as the substrate binding cleft in MibH. The CASTp server was used to identify residues delineating the proposed peptide binding site,[50] allowing the calculation of its solvent accessible surface area in PyMOL, which reveals this region to be 718.5 Å^2 larger than that of other members of this enzyme family. In addition, the greater relative hydrophobicity of the MibH binding cleft also supports its peptide substrate preference over free tryptophan (Figure 6b). We next performed a docking analysis of MibH and its substrate deschloro NAI-107. Docking poses were obtained where the C-5 indole carbon is in closest proximity to the catalytic Lys102 with an 8.5-Å distance to its ε-nitrogen (Supporting Information Figure S5). For catalysis to occur, we envision this distance to be reduced upon substrate binding.

To obtain further insights into the origins of the substrate specificity, a phylogenetic reconstruction using Maximum Likelihood methods (ML)[51] of different FADH$_2$-dependent halogenases that have been biochemically or structurally characterized was performed. Similar to recent results obtained in a phylogenetic study on the evolution of halogenases,[52] the ML tree revealed two main clades showing a strong correlation between the distribution of halogenases and their substrate specificity (Figure 7). One clade is formed by proteins known to halogenate pyrrole, phenyl, alkynyl, and alkyl groups of substrates tethered to a carrier (either a protein or coenzyme A; Figure 7, green).[41−44] These halogenases are present within assembly lines like nonribosomal peptide synthetase (NRPS) pathways and are responsible for halogenating a tethered building block that is subsequently incorporated into a final molecule.[41,42] MibH belongs to the same clade as Trp halogenases that halogenate free Trp, indicating it shares a closer evolutionary relationship with this type of enzymes. However, the early divergence of MibH from the other Trp halogenases perhaps reflects its preference to halogenate Trp embedded within a peptide substrate (Figure 7, blue). The phylogenetic inference displayed by these enzymes could prove to be helpful at predicting the substrate specificities of uncharacterized halogenases.

Conclusion. Here, we characterized two flavin-dependent enzymes involved in tailoring modifications during NAI-107
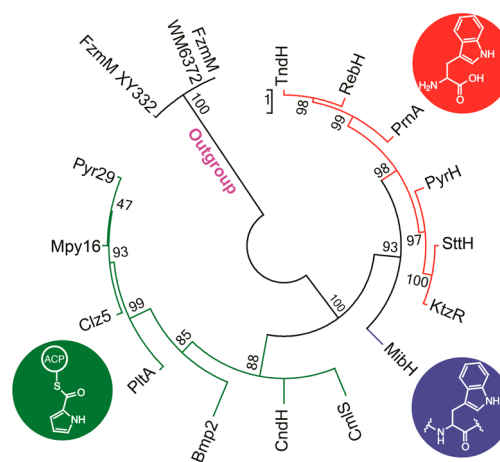

Figure 7. Maximum likelihood phylogenetic unrooted tree of various characterized flavin-dependent halogenases. Support for each clade is indicated by bootstrap percentage values. The name of each terminal branch corresponds to the name of the halogenase. Tree is colored based on substrate specificity. Green, halogenases that act on tethered substrates; blue, halogenases that act on peptides; red, halogenases that act on free Trp. Two flavin-dependent oxidoreductases were used as the outgroup.

biosynthesis, the FAD-dependent Cys decarboxylase MibD, and the FADH$_2$-dependent Trp halogenase MibH. MibD is shown to be specific for the C-terminal sequence of the precursor peptide MibA. Such specificity, coupled with the leader peptide-independent activity of this enzyme, could be exploited for the utilization of MibD in RiPP combinatorial biosynthesis by incorporating the MibD recognition sequence within the C-terminus of target peptides.

Similar to MibD, the Trp halogenase MibH also exhibited high substrate specificity. Prior mechanistic studies of FADH$_2$-dependent Trp halogenases provided evidence for the use of a covalent chloramine enzyme intermediate that can directly halogenate its substrate.[29] The use of such a covalent intermediate was proposed to facilitate regioselectivity. The decoupling of the site where the active halogenating agent is generated from the substrate-binding site was proposed to

assist in the evolution of catalysts with different substrate tolerance.[49] Although MibH functions on a peptide, where extensive interactions between catalysts and substrate may already establish regioselectivity, the active site features, including the Lys that is covalently modified, are largely conserved. These comparisons further support the theory that substrate specificities among different classes of FADH$_2$-dependent halogenases are likely due to changes only at the substrate-binding site, rather than at the site where the active chlorinating agent is produced. This strategy allows for these enzymes to not only use free Trp and Trp bound to carrier proteins as substrates but also allows them to act on peptides as exemplified by the lantibiotic halogenase MibH.

METHODS

***In Vitro* Reconstitution of MibD Activity and Characterization of Its Substrate Specificity.** His$_6$-MibD (10 μM) was incubated with 150 μM linear His$_6$-MibA at RT for 2 h in 100 μL of reaction buffer (20 mM Tris HCl pH 8.0, and 3 mM DTT). The reaction was purified using a C$_{18}$ zip-tip concentrator to remove excess salts, mixed in a 1:1 ratio with α-cyano-4-hydroxycinnamic acid and analyzed by MALDI-TOF MS using a Voyager-DE STR in positive mode. To determine the importance of the N-terminal leader sequence for oxidative decarboxylation, 80 μM linear His$_6$-MibA was incubated with trypsin in a 1:10 ratio (trypsin:peptide) in 100 μL of trypsin buffer (100 mM Tris HCl at pH 8.0, 5 mM TCEP, 2 mM MgCl$_2$) and incubated for 3 h at RT. Removal of the N-terminal leader sequence was monitored by MALDI-TOF MS analysis as described above. After complete N-terminal leader sequence removal, His$_6$-MibD (2 μM) was added to the reaction, and the solution was incubated for 15 min at RT. Analysis of the reaction was performed by MALDI-TOF MS as described above. To determine the localization of the post-translational modification, an aliquot of 10 μL of the reaction mixture was injected into an Acquity UPLC Phenomenex Jupiter C$_{18}$ column (5 μm, 0.1 × 150 mm) coupled to an electrospray ionization mass spectrometer (Q-TOF Synapt-G1 Waters in positive ion scan mode using the manufacturer's conditions for tandem MS/MS fragmentation). The sample was fractionated using a linear gradient from 2% (v/v) solvent A (0.1% (v/v) formic acid in acetonitrile) in 98% (v/v) solvent B (0.1% (v/v) formic acid in water) to 98% (v/v) solvent A over 20 min.

To characterize the substrate specificity of His$_6$-MibD, several lanthipeptide precursor peptides were used as substrates following the same reaction conditions as described above. Lanthipeptide precursor peptides ending in Cys (ProcA1.1, 1.7, and 2.8, Table S1) were obtained following previously described pocedures.[53] Oxidative decarboxylation was monitored by MALDI-TOF MS analysis using a Voyager-DE STR.

Reconstitution of MibH Activity *in Vitro* and Characterization of Its Substrate Specificity. MibH activity assays were performed in 20 mM sodium phosphate buffer at pH 7.4, 10 mM NaCl, 5 μM FAD, 5 μM His$_6$-MibS, 5 μM His$_6$-MibH, and 50 μM dechloromicrobisporicin. Reactions were initiated by the addition of 100 μM NADH. Halogenation assays were incubated at 30 °C for 2 h. After the incubation period, samples were centrifuged (13 000 × g, 10 min, 25 °C) to remove insoluble material and analyzed by LC/ESI-MS on an Acquity UPLC Phenomenex Jupiter C$_{18}$ column (5 μm, 0.1 × 150 mm) coupled to an electrospray ionization Q-TOF Synapt-G1 mass spectrometer (Waters) in positive ion mode. LC/ESI-Q/TOF MS and tandem MS conditions used were similar to the ones already described above. To characterize the substrate specificity of MibH, several substrates (Table 1) were tested for halogenation activity using similar reaction conditions as described above. Samples were then centrifuged to remove insoluble material and desalted using a C$_{18}$ zip-tip concentrator following standard procedures. An aliquot of the sample was mixed in a 1:1 ratio with 2,5-dihydroxybenzoic acid matrix, and the extent of halogenation was analyzed using a Bruker

UltrafleXtreme MALDI TOF-TOF mass spectrometer in positive mode.

MibH Structure Determination. Following purification of MibH by nickel affinity chromatography as described in the SI, the protein was desalted by size exclusion chromatography using a HiLoad 16/600 Superdex 200 column (flow rate of 1 mL min^{-1}) connected to an ÄKTA purifier at 4 °C (buffer of 20 mM HEPES at pH 8.0 and 150 mM KCl). Eluted protein was then concentrated to 22 mg mL^{-1} in the presence of 2 mM FAD prior to crystallization. Crystals were obtained within 24 h in hanging drops containing 12.5% MPD, 12.5% PEG 3.35K, 0.1 M MES/imidazole at pH 6.5, and 0.09 M NPS (1:1:1 NaNO$_3$, Na$_2$HPO4, (NH$_4$)$_2$SO$_4$). Prior to data collection, crystals were transferred into the crystallization solution supplemented with 20% MPD and vitrified in liquid nitrogen. Data were collected at the Advanced Photon Source, Argonne National Lab using the Life-Science Collaborative Access Team (LS-CAT) 21-ID-G beamline. Raw data were integrated and scaled using the autoPROC software.[54] The structure was determined by molecular replacement using the PHASER software[55] and a modified model of PyrH (PDB: 2WET) with all nonidentical residues truncated to Ala. The initial model was further improved using Buccaneer[56] and interspersed with rounds of manual building using COOT.[57] Interim models were routinely adjusted through rounds of crystallographic refinement using Refmac5.[58] Refinement converged to the final model for which statistics are presented in Supporting Information Table S2.

ASSOCIATED CONTENT

Ⓢ Supporting Information

The Supporting Information is available free of charge on the ACS Publications website at DOI: 10.1021/acschembio.6b01031.

> General methods and experimental details on the cloning, overexpression, and purification of the peptides and proteins used in this study; characterization of the cofactors bound to MibD and MibS; kinetic characterization of MibS; phylogenetic analysis of flavin dependent halogenases; isolation of **1**; chemical synthesis of peptide **3**; and generation of MibH-deschloro NAI-107 docking models (PDF)

Accession Codes

The structure factors and coordinates for the MibH structure have been deposited in the Protein Data Bank under the accession code 5UAO.

AUTHOR INFORMATION

Corresponding Authors
*Phone: 217-333-0641 E-mail: snair@illinois.edu.
*Phone: 217-244-5360 E-mail: vddonk@illinois.edu.
ORCID Ⓘ
Leif Smith: 0000-0002-0876-7260
Wilfred A. van der Donk: 0000-0002-5467-7071

Author Contributions

M.A.O. and W.A.V. designed experiments and analyzed biochemical data. M.A.O. performed biochemical and bioinformatic experiments. S.M. synthesized and characterized NAI-107$_{\Delta12-24}$. D.P.C. and S.K.N. performed and analyzed structural experiments. N.G. and B.L. cloned *mib* genes. G.N.T. provided prochlorosin precursor peptides. S.D., S.I.M., and M.S. provided *Microbispora* sp. 107891 and deschloromicrobisporicin. J.E. and L.S. provided mutacin 1140. M.A.O., W.A.V., D.P.C., and S.K.N. wrote the manuscript.

■ REFERENCES

(1) Arnison, P. G., Bibb, M. J., Bierbaum, G., Bowers, A. A., Bugni, T. S., Bulaj, G., Camarero, J. A., Campopiano, D. J., Challis, G. L., Clardy, J., Cotter, P. D., Craik, D. J., Dawson, M., Dittmann, E., Donadio, S., Dorrestein, P. C., Entian, K. D., Fischbach, M. A., Garavelli, J. S., Goransson, U., Gruber, C. W., Haft, D. H., Hemscheidt, T. K., Hertweck, C., Hill, C., Horswill, A. R., Jaspars, M., Kelly, W. L., Klinman, J. P., Kuipers, O. P., Link, A. J., Liu, W., Marahiel, M. A., Mitchell, D. A., Moll, G. N., Moore, B. S., Müller, R., Nair, S. K., Nes, I. F., Norris, G. E., Olivera, B. M., Onaka, H., Patchett, M. L., Piel, J., Reaney, M. J., Rebuffat, S., Ross, R. P., Sahl, H. G., Schmidt, E. W., Selsted, M. E., Severinov, K., Shen, B., Sivonen, K., Smith, L., Stein, T., Süssmuth, R. D., Tagg, J. R., Tang, G. L., Truman, A. W., Vederas, J. C., Walsh, C. T., Walton, J. D., Wenzel, S. C., Willey, J. M., and van der Donk, W. A. (2013) Ribosomally synthesized and post-translationally modified peptide natural products: overview and recommendations for a universal nomenclature. *Nat. Prod. Rep. 30*, 108–160.

(2) Ortega, M. A., and van der Donk, W. A. (2016) New insights into the biosynthetic logic of ribosomally synthesized and post-translationally modified peptide natural products. *Cell Chem. Biol. 23*, 31–44.

(3) Knerr, P. J., and van der Donk, W. A. (2012) Discovery, biosynthesis, and engineering of lantipeptides. *Annu. Rev. Biochem. 81*, 479–505.

(4) Bierbaum, G., and Sahl, H. G. (2009) Lantibiotics: mode of action, biosynthesis and bioengineering. *Curr. Pharm. Biotechnol. 10*, 2–18.

(5) Plat, A., Kuipers, A., Rink, R., and Moll, G. N. (2013) Mechanistic aspects of lanthipeptide leaders. *Curr. Protein Pept. Sci. 14*, 85–96.

(6) Oman, T. J., and van der Donk, W. A. (2010) Follow the leader: the use of leader peptides to guide natural product biosynthesis. *Nat. Chem. Biol. 6*, 9–18.

(7) Yang, X., and van der Donk, W. A. (2013) Ribosomally synthesized and post-translationally modified peptide natural products: new insights into the role of leader and core peptides during biosynthesis. *Chem. - Eur. J. 19*, 7662–7677.

(8) Velásquez, J. E., Zhang, X., and van der Donk, W. A. (2011) Biosynthesis of the antimicrobial peptide epilancin 15X and its unusual N-terminal lactate moiety. *Chem. Biol. 18*, 857–867.

(9) Castiglione, F., Lazzarini, A., Carrano, L., Corti, E., Ciciliato, I., Gastaldo, L., Candiani, P., Losi, D., Marinelli, F., Selva, E., and Parenti, F. (2008) Determining the structure and mode of action of microbisporicin, a potent lantibiotic active against multiresistant pathogens. *Chem. Biol. 15*, 22–31.

(10) Maffioli, S. I., Monciardini, P., Catacchio, B., Mazzetti, C., Munch, D., Brunati, C., Sahl, H. G., and Donadio, S. (2015) Family of class I lantibiotics from actinomycetes and improvement of their antibacterial activities. *ACS Chem. Biol. 10*, 1034–1042.

(11) Maffioli, S. I., Iorio, M., Sosio, M., Monciardini, P., Gaspari, E., and Donadio, S. (2014) Characterization of the congeners in the lantibiotic NAI-107 complex. *J. Nat. Prod. 77*, 79–84.

(12) Foulston, L. C., and Bibb, M. J. (2010) Microbisporicin gene cluster reveals unusual features of lantibiotic biosynthesis in actinomycetes. *Proc. Natl. Acad. Sci. U. S. A. 107*, 13461–13466.

(13) Münch, D., Müller, A., Schneider, T., Kohl, B., Wenzel, M., Bandow, J. E., Maffioli, S., Sosio, M., Donadio, S., Wimmer, R., and Sahl, H. G. (2014) The lantibiotic NAI-107 binds to bactoprenol-bound cell wall precursors and impairs membrane functions. *J. Biol. Chem. 289*, 12063–12076.

(14) Jabés, D., Brunati, C., Candiani, G., Riva, S., Romanó, G., and Donadio, S. (2011) Efficacy of the new lantibiotic NAI-107 in experimental infections induced by multidrug-resistant Gram-positive pathogens. *Antimicrob. Agents Chemother. 55*, 1671–1676.

(15) Maffioli, S. I., Cruz, J. C., Monciardini, P., Sosio, M., and Donadio, S. (2016) Advancing cell wall inhibitors towards clinical applications. *J. Ind. Microbiol. Biotechnol. 43*, 177–184.

(16) Foulston, L., and Bibb, M. (2011) Feed-forward regulation of microbisporicin biosynthesis in *Microbispora corallina*. *J. Bacteriol. 193*, 3064–3071.

(17) Ortega, M. A., Hao, Y., Walker, M. C., Donadio, S., Sosio, M., Nair, S. K., and van der Donk, W. A. (2016) Structure and tRNA specificity of MibB, a lantibiotic dehydratase from Actinobacteria involved in NAI-107 biosynthesis. *Cell Chem. Biol. 23*, 370–380.

(18) Kupke, T., Stevanovic, S., Sahl, H. G., and Götz, F. (1992) Purification and characterization of EpiD, a flavoprotein involved in the biosynthesis of the lantibiotic epidermin. *J. Bacteriol. 174*, 5354–5361.

(19) Majer, F., Schmid, D. G., Altena, K., Bierbaum, G., and Kupke, T. (2002) The flavoprotein MrsD catalyzes the oxidative decarboxylation reaction involved in formation of the peptidoglycan biosynthesis inhibitor mersacidin. *J. Bacteriol. 184*, 1234–1243.

(20) Kupke, T., Uebele, M., Schmid, D., Jung, G., Blaesse, M., and Steinbacher, S. (2000) Molecular characterization of lantibiotic-synthesizing enzyme EpiD reveals a function for bacterial Dfp proteins in coenzyme A biosynthesis. *J. Biol. Chem. 275*, 31838–31846.

(21) Strauss, E., Zhai, H., Brand, L. A., McLafferty, F. W., and Begley, T. P. (2004) Mechanistic studies on phosphopantothenoylcysteine decarboxylase: trapping of an enethiolate intermediate with a mechanism-based inactivating agent. *Biochemistry 43*, 15520–15533.

(22) Strauss, E., and Begley, T. P. (2001) Mechanistic studies on phosphopantothenoylcysteine decarboxylase. *J. Am. Chem. Soc. 123*, 6449–6450.

(23) Blaesse, M., Kupke, T., Huber, R., and Steinbacher, S. (2000) Crystal structure of the peptidyl-cysteine decarboxylase EpiD complexed with a pentapeptide substrate. *EMBO J. 19*, 6299–6310.

(24) Blaesse, M., Kupke, T., Huber, R., and Steinbacher, S. (2003) Structure of MrsD, an FAD-binding protein of the HFCD family. *Acta Crystallogr., Sect. D: Biol. Crystallogr. D59*, 1414–1421.

(25) Kempter, C., Kupke, T., Kaiser, D., Metzger, J. W., and Jung, G. (1996) Thioenols from peptidyl cysteines: oxidative decarboxylation of a 13C-labeled substrate. *Angew. Chem., Int. Ed. Engl. 35*, 2104–2107.

(26) Dong, C., Flecks, S., Unversucht, S., Haupt, C., van Pée, K. H., and Naismith, J. H. (2005) Tryptophan 7-halogenase (PrnA) structure suggests a mechanism for regioselective chlorination. *Science 309*, 2216–2219.

(27) Yeh, E., Garneau, S., and Walsh, C. T. (2005) Robust *in vitro* activity of RebF and RebH, a two-component reductase/halogenase, generating 7-chlorotryptophan during rebeccamycin biosynthesis. *Proc. Natl. Acad. Sci. U. S. A. 102*, 3960–3965.

(28) Yeh, E., Cole, L. J., Barr, E. W., Bollinger, J. M., Jr., Ballou, D. P., and Walsh, C. T. (2006) Flavin redox chemistry precedes substrate chlorination during the reaction of the flavin-dependent halogenase RebH. *Biochemistry 45*, 7904–7912.

(29) Yeh, E., Blasiak, L. C., Koglin, A., Drennan, C. L., and Walsh, C. T. (2007) Chlorination by a long-lived intermediate in the mechanism of flavin-dependent halogenases. *Biochemistry 46*, 1284–1292.

(30) Kupke, T., and Götz, F. (1997) The enethiolate anion reaction products of EpiD. pKa value of the enethiol side chain is lower than that of the thiol side chain of peptides. *J. Biol. Chem. 272*, 4759–4762.

(31) Kupke, T., Kempter, C., Gnau, V., Jung, G., and Götz, F. (1994) Mass spectroscopic analysis of a novel enzymatic reaction. Oxidative decarboxylation of the lantibiotic precursor peptide EpiA catalyzed by the flavoprotein EpiD. *J. Biol. Chem. 269*, 5653–5659.

(32) Kupke, T., Kempter, C., Jung, G., and Götz, F. (1995) Oxidative decarboxylation of peptides catalyzed by flavoprotein EpiD. Determi-

nation of substrate specificity using peptide libraries and neutral loss mass spectrometry. *J. Biol. Chem.* 270, 11282−11289.

(33) Escano, J., Stauffer, B., Brennan, J., Bullock, M., and Smith, L. (2015) Biosynthesis and transport of the lantibiotic mutacin 1140 produced by *Streptococcus mutans. J. Bacteriol.* 197, 1173−1184.

(34) Li, B., Sher, D., Kelly, L., Shi, Y., Huang, K., Knerr, P. J., Joewono, I., Rusch, D., Chisholm, S. W., and van der Donk, W. A. (2010) Catalytic promiscuity in the biosynthesis of cyclic peptide secondary metabolites in planktonic marine cyanobacteria. *Proc. Natl. Acad. Sci. U. S. A.* 107, 10430−10435.

(35) Gerlt, J. A., Bouvier, J. T., Davidson, D. B., Imker, H. J., Sadkhin, B., Slater, D. R., and Whalen, K. L. (2015) Enzyme Function Initiative-Enzyme Similarity Tool (EFI-EST): A web tool for generating protein sequence similarity networks. *Biochim. Biophys. Acta, Proteins Proteomics* 1854, 1019−1037.

(36) Li, B., and Walsh, C. T. (2010) Identification of the gene cluster for the dithiolopyrrolone antibiotic holomycin in *Streptomyces clavuligerus. Proc. Natl. Acad. Sci. U. S. A.* 107, 19731−19735.

(37) Brock, N. L., Nikolay, A., and Dickschat, J. S. (2014) Biosynthesis of the antibiotic tropodithietic acid by the marine bacterium *Phaeobacter inhibens. Chem. Commun.* 50, 5487−5489.

(38) Schmid, D. G., Majer, F., Kupke, T., and Jung, G. (2002) Electrospray ionization Fourier transform ion cyclotron resonance mass spectrometry to reveal the substrate specificity of the peptidyl-cysteine decarboxylase EpiD. *Rapid Commun. Mass Spectrom.* 16, 1779−1784.

(39) van Heel, A. J., Mu, D., Montalbán-López, M., Hendriks, D., and Kuipers, O. P. (2013) Designing and producing modified, new-to-nature peptides with antimicrobial activity by use of a combination of various lantibiotic modification enzymes. *ACS Synth. Biol.* 2, 397−404.

(40) Payne, J. T., Andorfer, M. C., and Lewis, J. C. (2013) Regioselective arene halogenation using the FAD-dependent halogenase RebH. *Angew. Chem., Int. Ed.* 52, 5271−5274.

(41) Dorrestein, P. C., Yeh, E., Garneau-Tsodikova, S., Kelleher, N. L., and Walsh, C. T. (2005) Dichlorination of a pyrrolyl-S-carrier protein by FADH2-dependent halogenase PltA during pyoluteorin biosynthesis. *Proc. Natl. Acad. Sci. U. S. A.* 102, 13843−13848.

(42) Podzelinska, K., Latimer, R., Bhattacharya, A., Vining, L. C., Zechel, D. L., and Jia, Z. (2010) Chloramphenicol biosynthesis: the structure of CmlS, a flavin-dependent halogenase showing a covalent flavin-aspartate bond. *J. Mol. Biol.* 397, 316−331.

(43) Agarwal, V., El Gamal, A. A., Yamanaka, K., Poth, D., Kersten, R. D., Schorn, M., Allen, E. E., and Moore, B. S. (2014) Biosynthesis of polybrominated aromatic organic compounds by marine bacteria. *Nat. Chem. Biol.* 10, 640−647.

(44) Buedenbender, S., Rachid, S., Müller, R., and Schulz, G. E. (2009) Structure and action of the myxobacterial chondrochloren halogenase CndH: a new variant of FAD-dependent halogenases. *J. Mol. Biol.* 385, 520−530.

(45) Smith, L., Zachariah, C., Thirumoorthy, R., Rocca, J., Novak, J., Hillman, J. D., and Edison, A. S. (2003) Structure and dynamics of the lantibiotic mutacin 1140. *Biochemistry* 42, 10372−10384.

(46) Chen, S., Wilson-Stanford, S., Cromwell, W., Hillman, J. D., Guerrero, A., Allen, C. A., Sorg, J. A., and Smith, L. (2013) Site-directed mutations in the lanthipeptide mutacin 1140. *Appl. Environ. Microbiol.* 79, 4015−4023.

(47) Flecks, S., Patallo, E. P., Zhu, X., Ernyei, A. J., Seifert, G., Schneider, A., Dong, C., Naismith, J. H., and van Pée, K. H. (2008) New insights into the mechanism of enzymatic chlorination of tryptophan. *Angew. Chem., Int. Ed.* 47, 9533−9536.

(48) Cruz, J. C., Iorio, M., Monciardini, P., Simone, M., Brunati, C., Gaspari, E., Maffioli, S. I., Wellington, E., Sosio, M., and Donadio, S. (2015) Brominated variant of the lantibiotic NAI-107 with enhanced antibacterial potency. *J. Nat. Prod.* 78, 2642−2647.

(49) Zhu, X., De Laurentis, W., Leang, K., Herrmann, J., Ihlefeld, K., van Pée, K. H., and Naismith, J. H. (2009) Structural insights into regioselectivity in the enzymatic chlorination of tryptophan. *J. Mol. Biol.* 391, 74−85.

(50) Dundas, J., Ouyang, Z., Tseng, J., Binkowski, A., Turpaz, Y., and Liang, J. (2006) CASTp: computed atlas of surface topography of proteins with structural and topographical mapping of functionally annotated residues. *Nucleic Acids Res.* 34, W116−118.

(51) Whelan, S., and Goldman, N. (2001) A general empirical model of protein evolution derived from multiple protein families using a maximum-likelihood approach. *Mol. Biol. Evol.* 18, 691−699.

(52) Xu, G., and Wang, B. G. (2016) Independent evolution of six families of halogenating enzymes. *PLoS One* 11, e0154619.

(53) Thibodeaux, G. N., and van der Donk, W. A. (2012) An engineered lantipeptide synthetase serves as a general leader peptide-dependent kinase. *Chem. Commun.* 48, 10615−10617.

(54) Vonrhein, C., Flensburg, C., Keller, P., Sharff, A., Smart, O., Paciorek, W., Womack, T., and Bricogne, G. (2011) Data processing and analysis with the autoPROC toolbox. *Acta Crystallogr., Sect. D: Biol. Crystallogr.* 67, 293−302.

(55) Bunkoczi, G., Echols, N., McCoy, A. J., Oeffner, R. D., Adams, P. D., and Read, R. J. (2013) Phaser.MRage: automated molecular replacement. *Acta Crystallogr., Sect. D: Biol. Crystallogr.* 69, 2276−2286.

(56) Cowtan, K. (2006) The Buccaneer software for automated model building. 1. Tracing protein chains. *Acta Crystallogr., Sect. D: Biol. Crystallogr.* 62, 1002−1011.

(57) Emsley, P., and Cowtan, K. (2004) Coot: model-building tools for molecular graphics. *Acta Crystallogr., Sect. D: Biol. Crystallogr.* 60, 2126−2132.

(58) Murshudov, G. N., Skubak, P., Lebedev, A. A., Pannu, N. S., Steiner, R. A., Nicholls, R. A., Winn, M. D., Long, F., and Vagin, A. A. (2011) REFMAC5 for the refinement of macromolecular crystal structures. *Acta Crystallogr., Sect. D: Biol. Crystallogr.* 67, 355−367.